3-DPTV Experiments of Anomalous, Steady Transport of a Conservative Tracer in Homogeneous and Heterogeneous Porous Media

by

A. Cenedese[†], J.H. Cushman[&] and M. Moroni[†]

[†]University of Rome "La Sapienza", DITS, Via Eudossiana 18, 00184 – Rome, Italy

[&]Center for Applied Math, Purdue University, 47907 W. Lafayette (IN-US)

ABSTRACT

Lagrangian theories of flow and transport in porous media are largely unverified experimentally. The flow field inside a porous medium is three-dimensional so a 3D imaging technique has to be adopted to detect tracer particle movements. We present an application of the "scanning" 3-DPVT, using two cameras with optical axes orthogonal and coplanar (Fig. 1). Matched index (of refraction) porous media that are homogeneous and heterogeneous at the bench scale have been constructed and different mean flow rates applied. The reconstructed trajectories allow computing velocity distributions, mean square displacements, velocity correlation coefficients and classical dispersion tensors. Comparisons among the velocity correlation coefficient are also presented. These preliminary results show that the velocity is more correlated in the heterogeneous system than in the homogeneous ones.

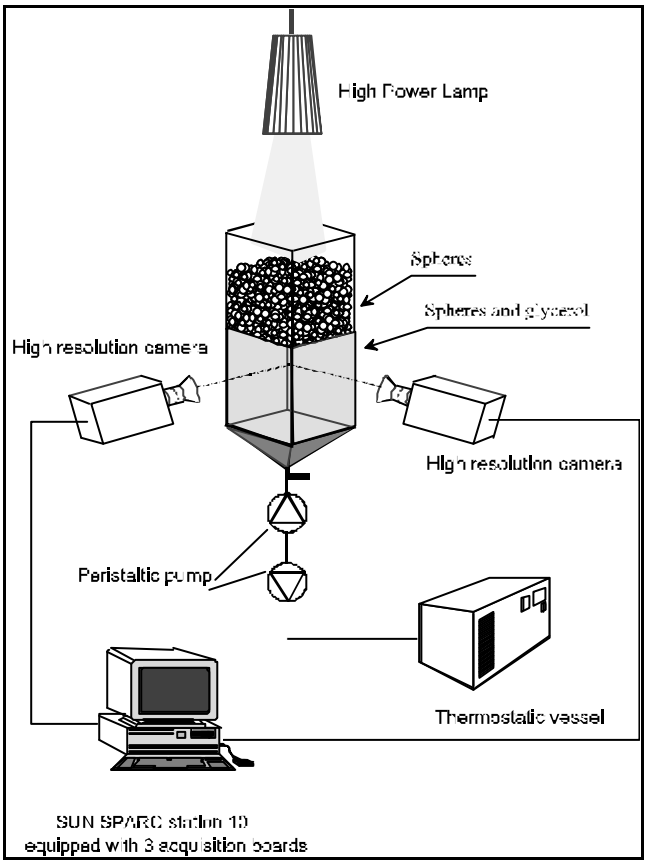

Fig. 1 Experimental set-up

INTRODUCTION

Fluids in porous media, though ubiquitous in nature and modern technologies, are notoriously difficult to study because they are "invisible" to most instrumentation. Consequently, theories of flow and transport in porous media are largely unverified experimentally. Though significant computational results exist on many scales (Bellin *et al*. 1996), these results are always based on the computer implementation of some approximation to reality. And as such, they may not mimic flow and transport in real porous media. Further, since we are interested in assessing the accuracy of transport models, only the velocity field (lagrangian or eulerian) or its statistics is required for our analysis. That is, it is not necessary to know, a priori or a posteriori, the hydraulic conductivity distribution. This gives us considerable freedom in designing the heterogeneous matrix and in constructing it in the flow cell. This is a significant advantage of our experimental approach over say a numerical Monte Carlo approach. In the latter, to obtain the velocity field, the conductivity distribution must be given a priori, and realizations generated and the velocity determined from the flow solution. Thus errors introduced in the numerical procedure of the flow problem propagate to the transport problem and transport models can not be examined independently of flow models.

To obtain the flow field inside a porous medium in three-dimensions, a 3D imaging technique must be adopted to detect tracer particle movements.

There are a number of imaging techniques for determining 3D trajectories in an observation volume (Stuer *et al*., 1999): (a) scanning (Guezennec *et al*., 1994); (b) defocusing (Willert and Gharib, 1992); (c) holographic (Hinsch and Hinrichs, 1996) and (d) stereoscopic (Maas, 1996).

Saleh *et al*. (1992), Cenedese and Viotti (1996) and Rashidi *et al* (1996) present applications of 2D imaging-based techniques to obtain velocities, trajectories, dispersion tensor components, and spatial averaged properties.

Other non-invasive techniques based on Positron Emission Tomography (PET) (Khalili *et al*. (1998)) or Magnetic Resonance Imaging (MRI) (Kutsovsky *et al*., 1996, Lebon *et al*. 1997, Park and Gibbs, 1999, Irwin *et al*., 1999) can be used for visualizing and making 3D quantitative measurements of transport through artificial or natural opaque permeable sediments, but these techniques do not supply individual tracer trajectories.

What we present is the application of the "scanning" 3-DPVT, performed with two cameras with optical axes orthogonal and coplanar.

Algorithms have been developed to analyze the images and to extract the 3-D trajectories. To this extent, the 2-dimensional trajectory projections reconstructed from the sequence of images captured from each camera are matched to get the 3-D displacements. The stereoscopic set-up has been carefully calibrated. The camera exterior and interior orientation parameters have to be estimated by placing three-dimensional targets. In this way, errors deriving from an unverified hypothesis of parallel optical rays can be corrected. As a consequence, the "exact" 3-D position of the particle can be ascertained. The reconstructed trajectories allow us to compute velocity distributions, mean square displacements, velocity correlation coefficients and the classical dispersion tensor.

1. HOMOGENEOUS POROUS MEDIA: EXPERIMENTAL SET-UP AND RESULTS

A matched index (of refraction) porous medium homogeneous at the bench scale has been constructed by filling a Perspex parallelepiped tank ($30\times30\times50$ cm^3) with 1.9 cm Pyrex spheres (Fig. 1). Four different mean flow rates were studied for the homogeneous case and the respective Reynolds numbers have been computed. Tab. 1 reports the Reynolds numbers characterising the present experiments, the mean velocities and the time and length integral scales. For further details see Moroni and Cushman (2000b).

The probability density functions (pdfs) of the transverse and longitudinal fluctuation velocity components have been evaluated and are shown in Figs. 2 and 3. The procedure adopted to compute the pdf and the comparison with others work can be found in Moroni and Cushman (2000a and 2000b).

	Vel1	Vel2	Vel3	Vel4

Re	0.049	0.085	0.105	0.129
Mean Velocity (cm/sec)	0.211	0.366	0.450	0.551
T_{xx} (sec)	1.87	1.80	1.52	1.41
T_{yy} (sec)	1.90	1.85	1.60	1.44
T_{zz} (sec)	4.80	4.40	3.80	1.71
L_{zz} (cm)	1.01	1.61	3.25	1.79

Tab. 1. Reynolds numbers, mean velocity and lagrangian integral scales for the four flow rates

Figures 4 and 5 show the non-dimensional lagrangian velocity correlation coefficient $\rho^*_{ij}(\tau)$. The lengths are made non-dimensional via the Pyrex bead diameter (d_{bead}), while the ratio between d_{bead} and the mean velocity (v_{mean}) is used as time scale. So

$$t^* = t/(d_{bead}/v_{mean}) \tag{1}$$

$$C^*_{ii} = C_{ii}/(d_{bead} \times d_{bead}) \qquad i = x, y, z \tag{2}$$

$$D^*_{ii} = D_{ii}/(d_{bead} \times v_{mean}) \qquad i = x, y, z \tag{3}$$

where C^*_{ii} is the non-dimensional displacement correlation coefficient and D^*_{ii} is the non-dimensional dispersion coefficient. D^*_{ii} is the inverse of the Peclet number.

Figures 4 and 5 show how the velocity correlation coefficients collapse onto the same curve. Only the slowest velocity (vel 1) presents an anomalous behaviour. The same conclusion can be drawn from Figs. 6, 7, 8, 9. Figure 6 shows the non-dimensional x, y-displacement correlation coefficients for different fluid velocities. Figure 7 shows the non-dimensional z-displacement correlation coefficients. Figure 8 displays the transverse components of the non-dimensional dispersion tensor for different flow rates. Finally Figure 9 reports the longitudinal component of the non-dimensional dispersion tensor.

The parameters used to obtain non-dimensional quantities seem to be appropriate, except for the slowest velocity. In particular, t^* represents the mean time that a particle needs to traverse a distance equal to d_{bead}.

Figure 4 shows that the transverse velocity correlation coefficients become uncorrelated after 4 bead diameters (except for vel1), while the longitudinal velocity correlation coefficient needs 6 bead diameters to become uncorrelated (Fig. 5).

It may be interesting to compare Figs. 4-5 and Figs. 8-9. The dispersion coefficient reaches zero after 2.5 t^*. This does not coincide with the decorrelation time (4 t^*). As shown in Moroni and Cushman (2000b), the dispersion coefficient was computed as follows:

$$D_{ij}(\tau) = \int_0^\tau < v'_i(t_0) v'_i(t_0 + \tau) > d\tau \tag{4}$$

From Fig. 4, we see the velocity correlation coefficients have a decreasing trend followed by an oscillating one. On the other hand, the asymptotic value for the dispersion coefficient in the transverse directions is not reached while the longitudinal component appears to go asymptotic. In the transverse directions the curves initially increase and then appear to decrease toward zero (zero is reached for t^*=2.5). Owing to the difficulties in obtaining long trajectories, the statistics degrade as the time interval increases. This is especially true in the transverse directions. The mismatch between the time of decorrelation and the time the zero value is reached can be justified considering that the asymptotic limit is reached.

Actually, we want to emphasise that the only true and acceptable value for the dispersion coefficient is the asymptotic one, that is the one corresponding to $\tau \to \infty$. The reason why we compute $D_{ij}(\tau)$ in the way we do is to see how the asymptotic limit is reached. A generalised approach of Cushman (1997) gives a theory capable of predicting this pre-asymptotic behaviour.

Comparing Figs. 5 and 9, we note that at t^*=6 the longitudinal velocity correlation coefficient is zero and the dispersion coefficient is asymptotic.

We conclude that the dispersion phenomenon in the transverse direction has a characteristic length scale of the dimension of two bead diameters, while in the longitudinal direction the length scale is six bead diameters.

If we introduce the Peclet number (Pe), where $Pe=(v_{mean} x d_{bead}/D)$ and D is the dispersion coefficient, we can notice that the plots in Figg. 8 and 9 report the behaviour of 1/Pe over t^*. Figure 10 displays Pe in the longitudinal direction as a function of t^*. The plot shows as Pe decreases as the non-dimensional time increases. There is a fair overlap between the curve characterising the different velocities. The Peclet number decreases with t^* until a constant value (approximately equal to 3) is reached.

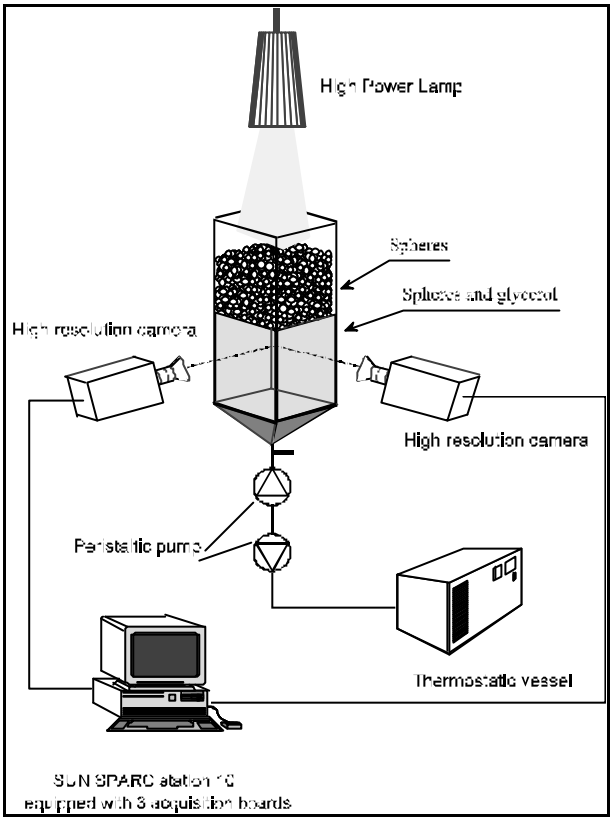

Fig. 1 Experimental set-up

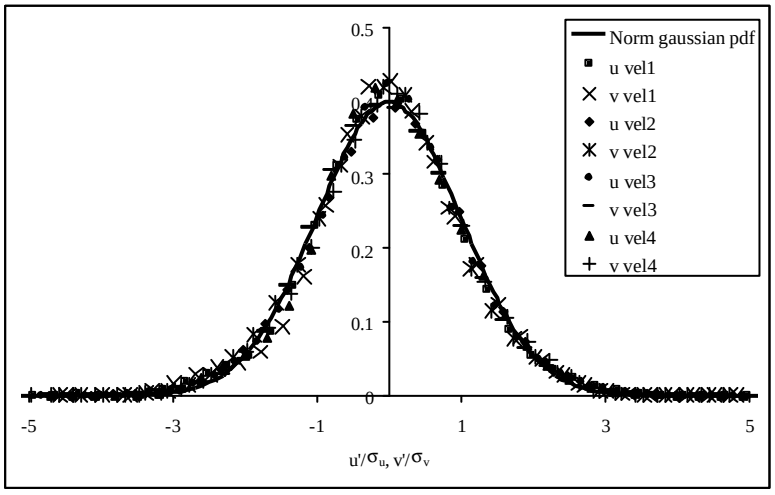

Fig. 2 Transverse velocity components pdfs

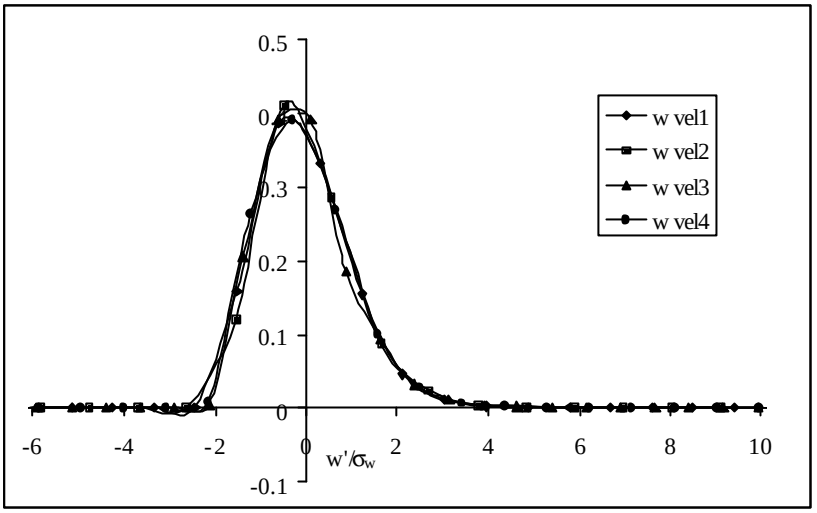

Fig. 3 Longitudinal velocity component pdfs

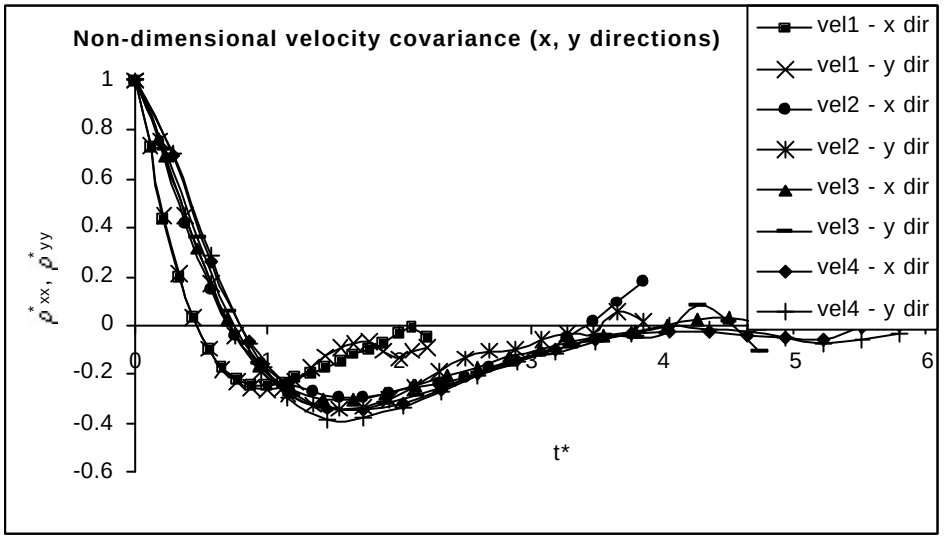

Fig. 4 Transverse velocity correlation coefficients for different flow rates (vel1<vel2<vel3<vel4)

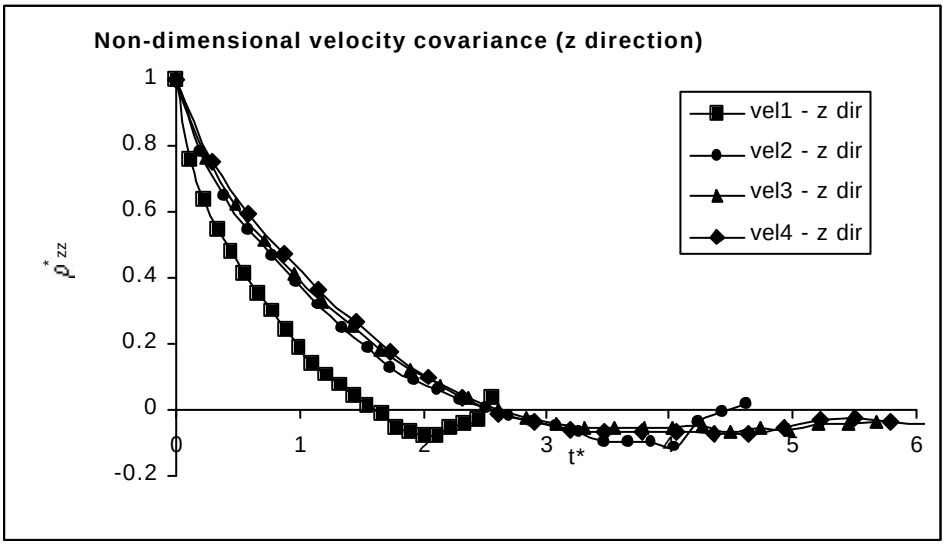

Fig. 5 Longitudinal velocity correlation coefficient for different flow rates (vel1<vel2<vel3<vel4)

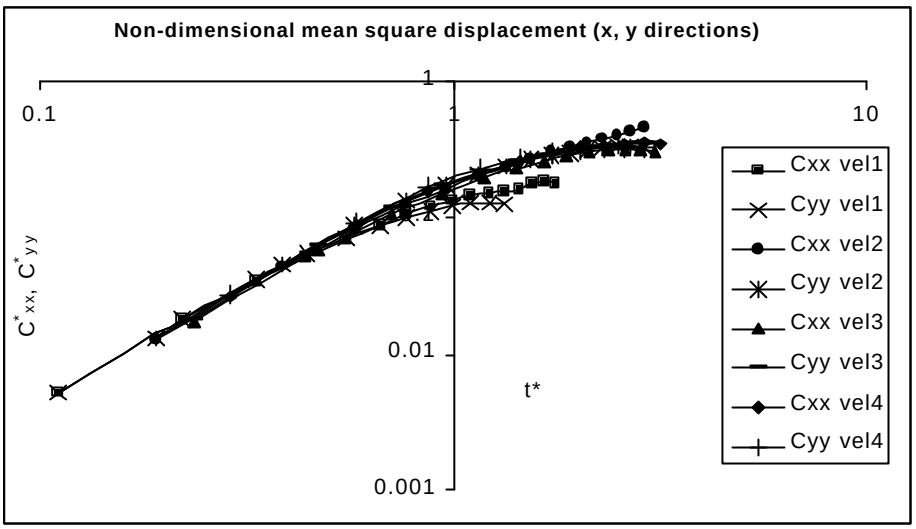

Fig. 6 Non-dimensional x, y-displacement correlation coefficients for different fluid velocities

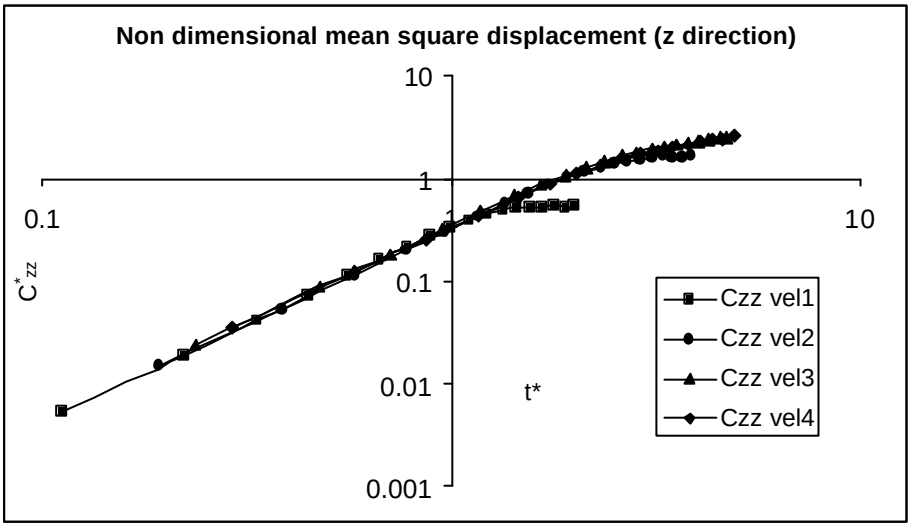

Fig. 7 Non-dimensional z-displacement correlation coefficients for different fluid velocities

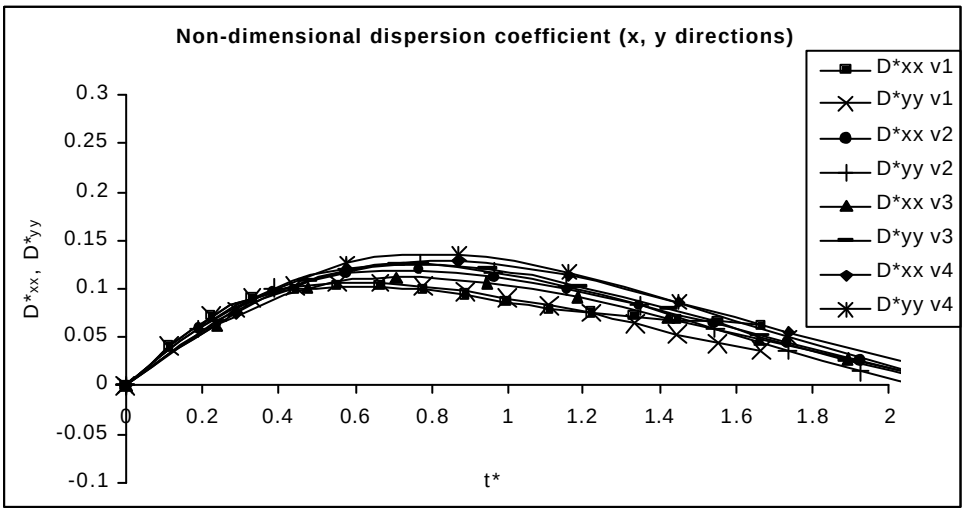

Fig. 8 Transverse components of the non-dimensional dispersion tensor for different flow rates

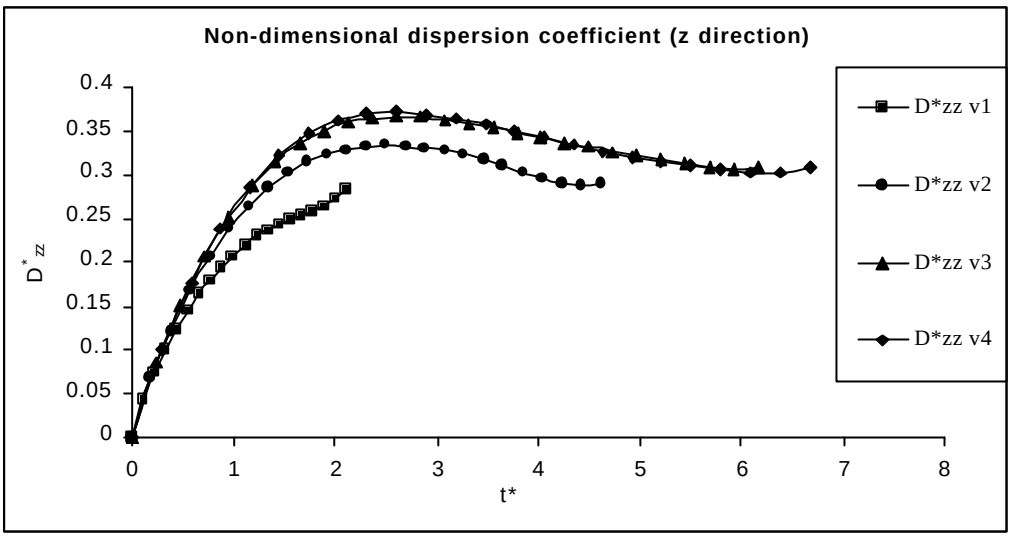

Fig. 9 Longitudinal component of the non-dimensional dispersion tensor for different flow rates

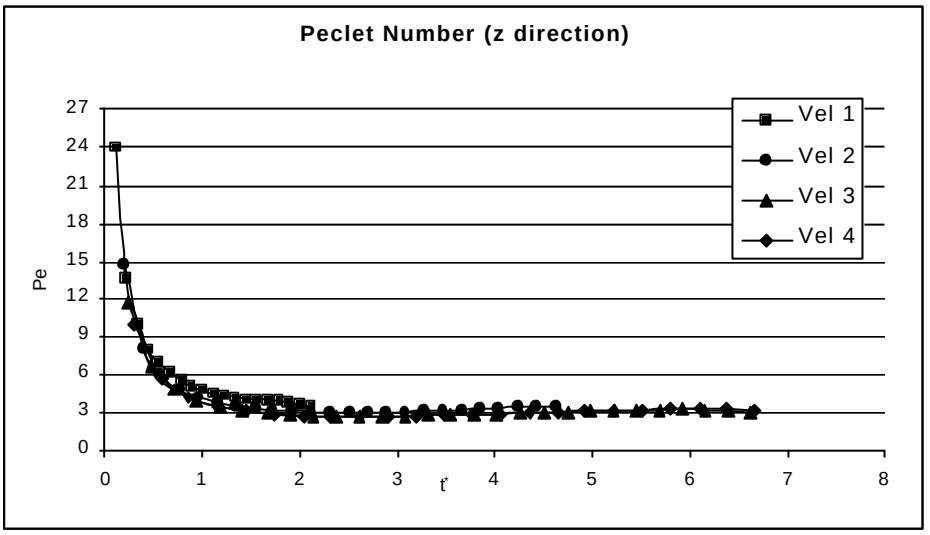

Fig. 10 Peclet number for different flow rates

2. HETEROGENEOUS POROUS MEDIA: EXPERIMENTAL SET-UP AND RESULTS

Five porous media which are heterogeneous at the laboratory scale have been constructed by placing Pyrex cylindrical beads of 0.4, 0.7, 1.0 cm as diameter and 1.9 cm Pyrex spheres in a $10\times10\times50$ cm^3 Perspex test section. Three mean flow rates were used and the respective Reynolds numbers have been computed.

Figure 11 shows the five kinds of heterogeneity we have realised.

We emphasise that Heterogeneities "2" and "3" have been modified after the first run of each series of experiments and the subsequent porous media were different than the one displays in Fig. 11. The large head losses caused by the smallest beads forced the porous matrix to swell when the glycerol was introduced. By studying the final distribution of the beads, we found the formation of lenses. So, 0.4 cm bead lenses were incorporated into 0.7 and 1.0 cm bead beds.

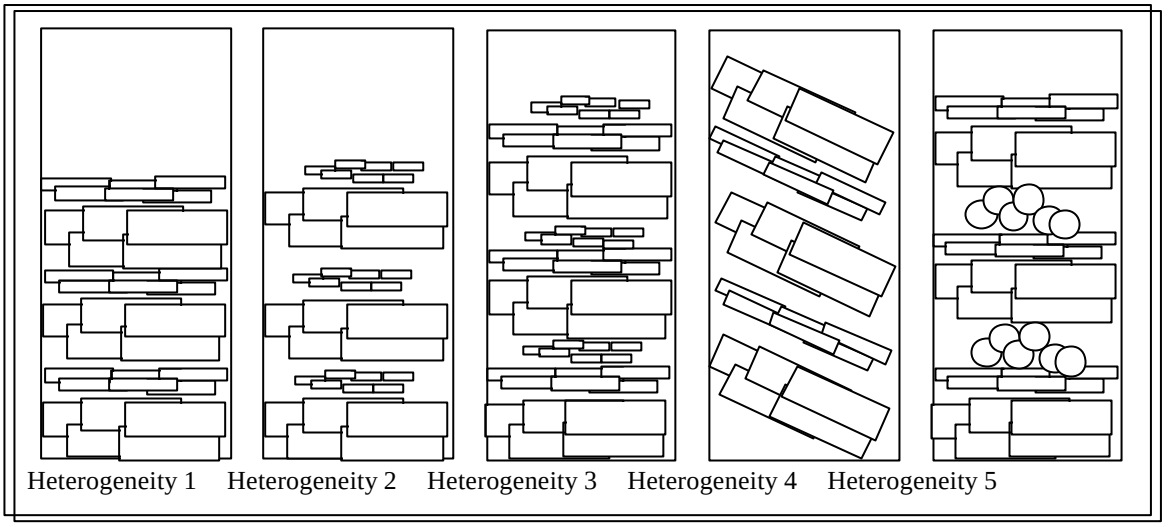

Fig. 11 Simulated heterogeneity (*f=0.4 cm,* *f=0.7 cm,* *f=1.0 cm,* *f=1.9 cm)*

Preliminary results concerning "Heterogeneity 1" and "Heterogeneity 4" will be presented. The aim of the analysis is to understand the behaviour of the velocity correlation coefficients, both in the transverse and in the longitudinal directions, with different kinds of heterogeneity. Further, we have compared the results of Cenedese and Viotti (1996) with the present ones. Cenedese and Viotti present the results of an experimental investigation of the dispersion phenomenon inside porous media via 2D-PTV (2D Particle Tracking Velocimetry). The media were constructed with 0.4 cm and 1.0 cm diameter beads, and were homogeneous at the bench scale.

We obtained non-dimensional data using the mean velocity and the bead diameters reported in Tab. 1 of Cenedese and Viotti (1996) and in the following Tab. 2.

Heterogeneity 1	v_{mean}= 0.257 cm/sec	d_{mean}= 0.85 cm
Heterogeneity 4	v_{mean}= 0.280 cm/sec	d_{mean}= 0.85 cm

Tab. 2 Parameters for non- dimensional velocity correlation coefficients

The mean dimension is obtained as an arithmetic average of the diameters of the two kinds of beads utilised (1.0 cm and 0.7 cm).

Figures 12 and 13 compare the velocity correlation coefficients characterising Heterogeneities 1 and 4. Both the figures show a higher correlation for velocities in Heterogeneity 4. One explanation is the anisotropy of medium 4 causes a continuous re-correlation of the velocity. The same effect is present for the other heterogeneous medium (this will be clearer when we will comment Figures 14 and 15), but it is more evident for the Heterogeneity 4.

Figures 14 and 15 compare homogeneous and heterogeneous velocity correlation coefficients.

There results illustrates how velocity is more correlated in the heterogeneous system than in the homogeneous ones. The different cases correspond to the series of Cenedese and Viotti (1996).

In passing we mentioned that the velocity correlation coefficients were computer in the same fashion for both the heterogeneous and homogeneous systems over all trajectories irrespective of origin.

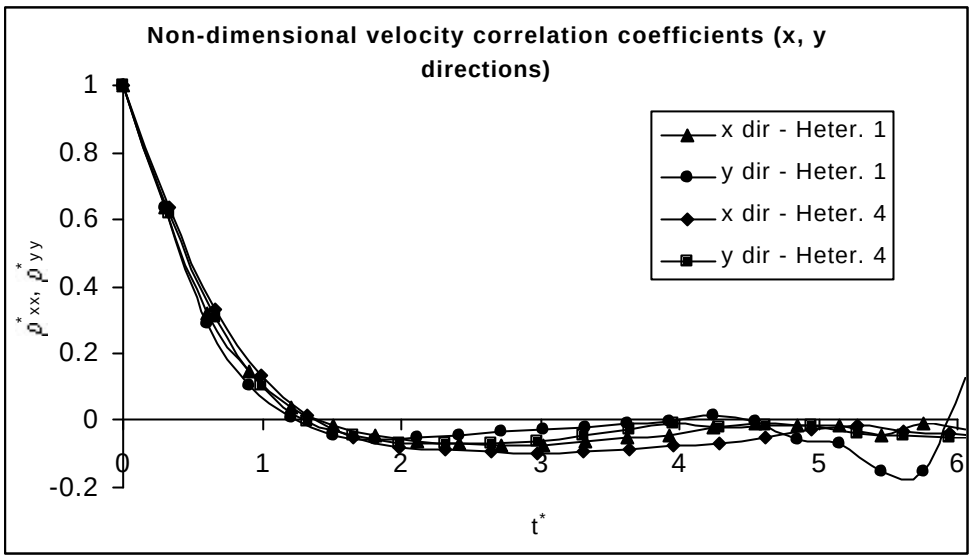

Fig. 12 Non-dimensional velocity correlation coefficient in the transverse directions for Heterogeneities 1 and 4

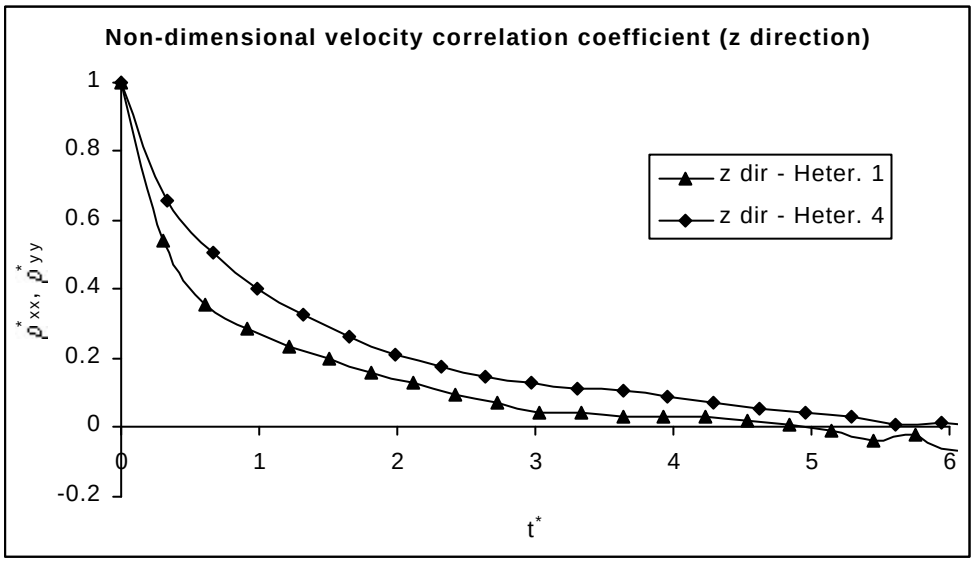

Fig. 13 Non-dimensional velocity correlation coefficient in the longitudinal direction for Heterogeneity 1 and 4

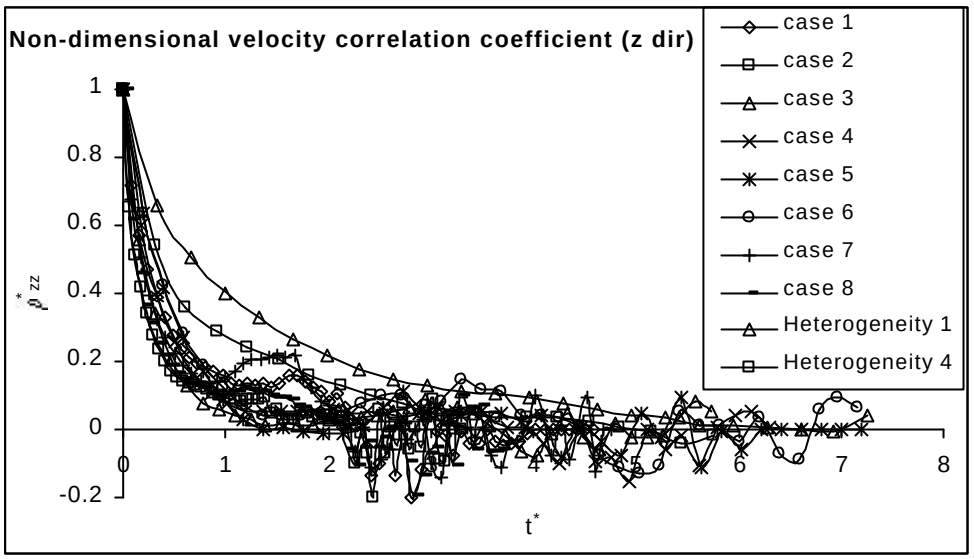

Fig. 14 Non-dimensional velocity correlation coefficient in the longitudinal direction: comparison between homogeneous media and Heterogeneity 1 and 4

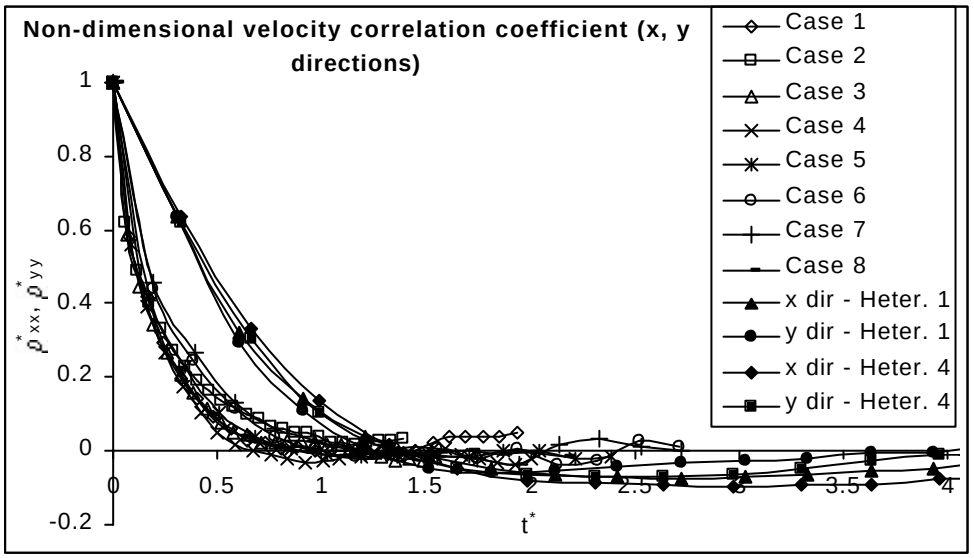

Fig. 15 Non-dimensional velocity correlation coefficient in the transverse directions: comparison between homogeneous media and Heterogeneity 1 and 4

REFERENCES

Cenedese A. & Viotti P., 1996, *"Lagrangian analysis of nonreactive pollutant dispersion in porous media by means of the particle Image Velocimetry Technique"*, Water Resour. Res. 32(8), 2329-2343;

Cushman H. J., 1997, *The physics of Fluids in Hierarchical Porous Media: Angstroms to Miles*, Kluwer Academic Publishers, The Netherlands;

Dagan G., 1989, *Flow and Transport in Porous Formations*, Springer-Verlag eds;

Guezennec Y. G., Brodkey R. S., Trigui N. & Kent J. C., 1994, *"Algorithms for fully automated three-dimensional Particle Tracking Velocimetry"*, Exp. Fluids, 17, 209-219;

Hinsch K.D. & Hinrichs H., 1996, *"Three-dimensional Particle Velocimetry"*, in Three-Dimensional Velocity and Vorticity Measuring and Image Analysis Technique, ed. Th. Dracos, Kluwer Academic Publishers;

Irwin N.C., Greenkorn R.A., Altobelli S.A. & Cushman J.H., 1999, *"Examination of Transport Theory of Arbitrary Order in Velocity Variance by MNR"*, AIChE J. 45(6);

Khalili A., Basu A. J. & Pietrzyk U., 1998, *"Flow visualization in porous media via Positron Emission Tomography"*, Phys. Fluids, 10 (4), 1031-1033;
Kutsovsky Y. E., Scriven L. E. & Davis H. T., 1996, *"NMR imaging of velocity profiles and velocity distributions in bead packs"*, Phys. Fluids, 8 (4), 863-871;
Lebon L., Leblond J. & Hulin J. P., *"Experimental measurements of dispersion processes at short times using a pulsed field gradient NMR technique"*, Phys. Fluids, 9 (3), 481-490 (1997);
Mass H.G., *"Contributions of digital photogrammetry to 3-D PTV"*, 1996, in Three-Dimensional Velocity and Vorticity Measuring and Image Analysis Techniques ed. Th. Dracos, Kluwer Academic Publishers;
Moroni M. & Cushman J. H., 2000a, *"3-DPTV Comparison with Statistical Mechanical Theories of Steady Conservative Tracer Transport in Porous Media"*, submitted to *Phys. Fluids*;
Moroni M. & Cushman J. H., 2000b, *"3D-PTV Studies of Asymptotic limits to Classical Stochastic Theories of Porous Media Transport"*, submitted to Water Resour. Res.;
Moroni M. and Cushman J.H., 2000, *"Statistical mechanical theories of multiscale transport and comparison with 3D-PTV experiments of the asymptotic limit"* submitted to *Phys. Fluids*;
Park J. & Gibbs S., 1999, *"Mapping Flow and Dispersion in a Packed Column by MRI"*, AIChE J, 45 (3), 655-660;
Rashidi M., Peurrung L., Tompson A.F.B. & Kulp T. J., 1996, *"Experimental analysis of pore-scale flow and transport in porous media"*, Adv. Water Resour., 19(3), 163-180;
Saleh S., Thovert J. F. & Adler P. M., 1993, *"Flow along porous-media by partial Image Velocimetry"* AIChE J, 39 (11) 1765-1776;
Stuer H., Maas H.G., Virant M. & Becker J., 1999, *"A volumetric 3D measurement tool for velocity field diagnostics in microgravity experiments"*, Meas. Sci. Technol. 10, 904-913;
Udrea D. D., Bryanston-Cross P. J., Querzoli G. & Moroni M., 1998, *"Particle Tracking Velocimetry techniques"*, Fluid Mechanics and its Application, Kluwer Academic;
Willert C.E. & Gharib M., 1992, *"Three-dimensional particle imaging with a single camera"*, Exp. Fluids 12, 353-358.